Grating dynamics in a photorefractive polymer with Alq_3 electron traps

C. W. Christenson[1,*], J. Thomas[1], P.-A. Blanche[1], R. Voorakaranam[1], R. A. Norwood[1], M. Yamamoto[2], and N. Peyghambarian[1]

[1]*College of Optical Sciences, The University of Arizona, Tucson, AZ 85721, USA*
[2]*Nitto Denko Technical, Oceanside, CA 92058, USA*
**cchristenson@optics.arizona.edu*

Abstract: The electron transporting molecule tris(8-hydroxyquinoline) aluminum (Alq_3) was added in low concentrations to a photorefractive polymer composite to provide trapping sites for electrons. This sample exhibited larger two-beam coupling gain, higher diffraction efficiency at lower voltages, and an increased dielectric breakdown strength compared to a control sample. The dynamics also revealed the presence of a competing grating, and a bipolar charge transport model is shown to fit the data. Overall, Alq_3 improves the response time, efficiency, and breakdown voltage without a significant increase in absorption or loss of phase stability. This has applications for reflection displays and pulsed writing, where charge trapping and generation are major factors limiting the usefulness of photorefractive polymers.

OCIS codes: (160.5320) Photorefractive materials; (050.7330) Volume gratings; (160.4890) Organic materials.

References and links

1. S. Ducharme, J. C. Scott, R. J. Twieg, and W. E. Moerner, "Observation of the photorefractive effect in a polymer," Phys. Rev. Lett. **66**(14), 1846–1849 (1991).
2. J. Thomas, R. A. Norwood, and N. Peyghambarian, "Photorefractive Polymers for Dynamic Holography," in *New Directions in Holography and Speckle*, H. J. Caulfield and C. S. Vikram, eds. (American Scientific, 2008).
3. B. L. Volodin, B. Kippelen, K. Meerholz, B. Javidi, and N. Peyghambarian, "Polymer optical pattern-recognition system for security verification," Nature **383**(6595), 58–60 (1996).
4. J. G. Winiarz, F. Ghebremichael, J. Thomas, G. Meredith, and N. Peyghambarian, "Dynamic correction of a distorted image using a photorefractive polymeric composite," Opt. Express **12**(11), 2517–2528 (2004).
5. S. Tay, J. Thomas, M. Eralp, G. Li, B. Kippelen, S. R. Marder, G. Meredith, A. Schülzgen, and N. Peyghambarian, "Photorefractive polymer composite operating at the optical communication wavelength of 1550nm," Appl. Phys. Lett. **85**(20), 4561–4563 (2004).
6. M. Salvador, J. Prauzner, S. Köber, K. Meerholz, J. J. Turek, K. Jeong, and D. D. Nolte, "Thee-dimensional holographic imaging of living tissue using a highly sensitive photorefractive polymer device," Opt. Express **17**(14), 11834–11849 (2009).
7. S. Tay, P.-A. Blanche, R. Voorakaranam, A. V. Tunç, W. Lin, S. Rokutanda, T. Gu, D. Flores, P. Wang, G. Li, P. St Hilaire, J. Thomas, R. A. Norwood, M. Yamamoto, and N. Peyghambarian, "An updatable holographic three-dimensional display," Nature **451**(7179), 694–698 (2008).
8. P.-A. Blanche, S. Tay, R. Voorakaranam, P. Saint-Hilaire, C. Christenson, T. Gu, W. Lin, D. Flores, P. Wang, M. Yamamoto, J. Thomas, R. A. Norwood, and N. Peyghambarian, "An updatable holographic display for 3D visualization," J. Disp. Technol. **4**(4), 424–430 (2008).
9. K. Meerholz, B. L. Volodin, B. Sandalphon, B. Kippelen, and N. Peyghambarian, "A photorefractive polymer with high optical gain and diffraction efficiency near 100%," Nature **371**(6497), 497–500 (1994).
10. M. Eralp, J. Thomas, S. Tay, G. Li, A. Schülzgen, R. A. Norwood, M. Yamamoto, and N. Peyghambarian, "Submillisecond response of a photorefractive polymer under single nanosecond pulse exposure," Appl. Phys. Lett. **89**(11), 114105 (2006).
11. J. Thomas, R. A. Norwood, and N. Peyghambarian, "Non-linear optical polymers for photorefractive applications," J. Mater. Chem. **19**(40), 7476–7489 (2009).
12. G. G. Malliaras, V. V. Krasnikov, H. J. Bolink, and G. Hadziioannou, "Control of charge trapping in a photorefractive polymer," Appl. Phys. Lett. **66**(9), 1038–1040 (1995).
13. O. Ostroverkhova, and K. D. Singer, "Space-charge dynamics in photorefractive polymers," J. Appl. Phys. **92**(4), 1727–1743 (2002).
14. J.-W. Oh, C. Lee, and N. Kim, "The effect of trap density on the space charge formation in polymeric photorefractive composites," J. Chem. Phys. **130**(13), 134909 (2009).

#123567 - $15.00 USD Received 29 Jan 2010; revised 7 Apr 2010; accepted 12 Apr 2010; published 20 Apr 2010

15. J. Zhang, J. Chen, Y. Liu, M. Huang, Q. Wei, and Q. Gong, "Improvement on the photorefractive performance of a monolithic molecular material by introducing electron traps," Appl. Phys. Lett. **85**(8), 1323–1325 (2004).
16. Q. Wei, Y. Liu, Z. Chen, M. Huang, J. Zhang, Q. Gong, X. Chen, and Q. Zhou, "Improvement in the photorefractivity of a polymeric composite doped with the electron-injecting material Alq_3," J. Opt. A, Pure Appl. Opt. **6**(9), 890–893 (2004).
17. J. Thomas, C. Fuentes-Hernandez, M. Yamamoto, K. Cammack, K. Matsumoto, G. A. Walker, S. Barlow, B. Kippelen, G. Meredith, S. R. Marder, and N. Peyghambarian, "Bistriarylamine polymer-based composites for photorefractive applications," Adv. Mater. **16**(22), 2032–2036 (2004).
18. A. Grunnet-Jepsen, C. L. Thompson, R. J. Twieg, and W. E. Moerner, "Amplified scattering in a high-gain photorefractive polymer," J. Opt. Soc. Am. B **15**(2), 901–904 (1998).
19. S. Zhivkova, and M. Miteva, "Holographic recording in photorefractive crystals with simultaneous electron-hole transport and two active centers," J. Appl. Phys. **68**(7), 3099–3103 (1990).
20. S. M. Silence, C. A. Walsh, J. C. Scott, T. J. Matray, R. J. Twieg, F. Hache, G. C. Bjorklund, and W. E. Moerner, "Subsecond grating growth in a photorefractive polymer," Opt. Lett. **17**(16), 1107–1109 (1992).
21. L. Wang, M.-K. Ng, and L. Yu, "Photorefraction and complementary grating competition in bipolar transport molecular material," Phys. Rev. B **62**(8), 4973–4984 (2000).
22. M. C. Bashaw, T.-P. Ma, R. C. Barker, S. Mroczkowski, and R. R. Dube, "Theory of complementary holograms arising from electron-hole transport in photorefractive media," J. Opt. Soc. Am. B **7**(12), 2329–2338 (1990).
23. Y. Ohmori, A. Fujii, M. Uchida, C. Morishima, and K. Yoshino, "Fabrication and optical characteristics of an organic multi-layer structure utilizing 8-hydroxyquinoline aluminium/aromatic diamine and its application for an electroluminescent diode," J. Phys. Condens. Matter **5**(43), 7979–7986 (1993).
24. T. R. Ohno, Y. Chen, S. Harvey, G. Kroll, J. Weaver, R. Haufler, and R. Smalley, "C_{60} bonding and energy-level alignment on metal and seminconductor surfaces," Phys. Rev. B **44**(24), 13747–13755 (1991).

1. Introduction

Since the first discovery of the photorefractive (PR) effect in polymers [1], a wide range of applications have been studied [2], such as optical correlation [3], beam cleanup [4], communication [5], tissue imaging [6], and dynamic holographic displays [7,8]. PR polymers have gained interest due to their high optical nonlinearity compared to inorganic materials, as well as low cost, ease of fabrication, and tunability of optical and electronic properties. Large diffraction efficiency, fast response time, and long persistence [8–11] have all been demonstrated in organic polymer composites.

In the PR effect, a modulation of the refractive index is induced which mimics the interference pattern of two coherent light beams. Charge generation, transport, and trapping lead to the development of space-charge (SC) field, and alignment of nonlinear and/or birefringent molecules in this field creates the macroscopic index modulation.

Many studies have been conducted on the effects of trap density and depth on PR performance [12–14]. In particular, it has been shown [15,16] that the addition of Alq_3 increases the two-beam coupling (TBC) gain and response time by acting as a trap for electrons, which increases the magnitude and speed of charge separation. Here, we report that the addition of Alq_3 leads to the development of a competing grating, as well as significant improvements in the steady-state diffraction efficiency and rise time. A bipolar charge transport model is shown to fit the data and the physical mechanisms are discussed. The advantages provided by Alq_3 are anticipated to be useful for updateable displays, where speed and high efficiency are essential to the success of applications such as medical imaging, data mining, and command-and-control.

2. Experiment

The PR composites studied contained the polymer host matrix poly(acrylic tetraphenyldiaminobiphenyl) (PATPD), which has a polyacrylate backbone with the well-known hole-transporting tetraphenyldiaminobiphenyl-type (TPD) pendant group attached through an alkoxy linker [17]. The chromophore 4-homopiperidinobenzylidenemalononitrile (7-DCST) was added to provide a refractive index change, but also acts as a sensitizer at 532nm, though C_{60} was the primary sensitizer. N-ethyl carbazole (ECZ) was included to act as a plasticizer. In one sample, Alq_3 was included at 1 wt%, an approximately optimal concentration for providing trapping sites for electrons generated through the photorefractive process, while still preventing bulk electron transport in the Alq_3 itself. Larger concentrations (1.5-2.0 wt%) tended to phase separate quickly, making the measurements unrepeatable. The

#123567 - $15.00 USD Received 29 Jan 2010; revised 7 Apr 2010; accepted 12 Apr 2010; published 20 Apr 2010

compositions of the two samples studied are shown in Table 1. The samples were prepared by melt processing the mixture between two indium-tin-oxide coated glass slides, with 105μm spacer beads used to fix the thickness. The absorption coefficient of each sample at 532nm and 633nm was approximately 160cm^{-1} and 45cm^{-1}, respectively. Both samples exhibited phase stability for several months at room temperature.

Table 1. Weight percentage of each component in the samples studied

Label	PATPD	7-DCST	ECZ	C_{60}	Alq_3
A	54.5	30	15	0.5	0.0
B	53.5	30	15	0.5	1.0

Degenerate four-wave mixing (DFWM) measurements were performed at 532nm to take advantage of the sensitization from 7-DCST. Each writing beam was *s*-polarized and incident on the sample with 100mW/cm^2. The external angle between the beams was 36° and the sample was tilted 55° relative to the bisector. The reading beam was *p*-polarized with an intensity of 1mW/cm^2 and aligned to be counter-propagating. Steady-state efficiency was measured by ramping the voltage up at 25V/sec and continuously monitoring the reading beam. To measure the transient behavior, a constant voltage was applied and the reading beam monitored the grating buildup as the writing beams were turned on and off, the total recording time being about 4 minutes.

TBC measurements were performed in the same geometry as DFWM, except no reading beam was present and the writing beams were *p*-polarized. The polarity of the electric field was set to minimize beam fanning [18]. 633nm light was used as the increased absorption at 532nm and the polarization introduced a prohibitive amount of beam fanning. This allowed an increase of the intensity to 1W/cm^2, since the samples were less vulnerable to high power at 633nm owing to the lower absorption coefficient there.

Photoconductivity was also measured at 532nm. The voltage was applied in the dark for 10-20min until the dark current reached steady-state, then the sample was illuminated until the current again leveled out.

3. Results

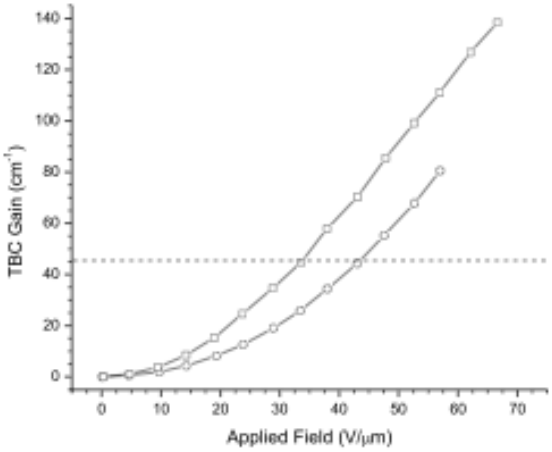

Fig. 1. TBC versus electric field for Samples A (circles) and B (squares). The horizontal dashed line indicates the absorption loss in each sample at 633nm.

The TBC results are shown in Fig. 1. The addition of Alq_3 improved the magnitude of the gain at all voltages; at 60V/μm there is a 75% increase in the net gain. Additionally, the Alq_3

#123567 - $15.00 USD Received 29 Jan 2010; revised 7 Apr 2010; accepted 12 Apr 2010; published 20 Apr 2010

tends to increase the dielectric breakdown strength, allowing larger voltages to be applied. The net gain of Sample B at 70V/μm was 89cm^{-1}, while at 532nm, no net gain was observed up to this voltage due to the large scattering losses. This could be attributed to the increased magnitude of the SC field due to more charge separation, however the TBC gain is affected by both the magnitude and phase of the SC field. DFWM is only directly affected by the former, and those results are shown in Fig. 2.

The improvement in the material response is significant. While no over-modulation peak was observed in Sample A up to 60V/μm, the addition of Alq_3 pushes the over-modulation down at least 20V/μm. Figure 3 shows the transient response for Sample B (70V/μm) and Sample A (60V/μm). Sample A rises to 67% of the steady-state value in about 40s, while it takes Sample B only 200ms, a difference too large to be attributed to the small difference in voltage. Sample B also exhibits recovery after about 30s of decay, which eventually turned around and started to decay again after 10-20min of observation. The decay for Sample A was measured for about 10mins without any sign of recovery.

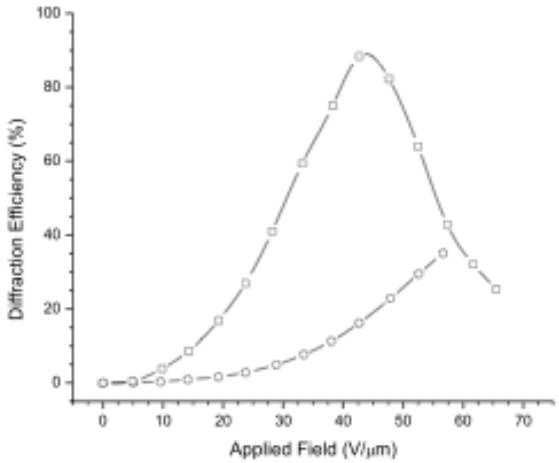

Fig. 2. Steady-state diffraction efficiency from DFWM measurements for Samples A (circles) and B(squares) at 532nm.

At Alq_3 concentrations of 1.5 wt% and above the composition was not phase stable, or would separate very quickly, precluding the possibility of measurements. Though up to at least 10 wt%, the breakdown strength remained. At 0.1 wt%, there was no observed difference with Sample A. This suggests there is window from above 0.1 to below 1.5 wt% where the dynamics can be altered without affecting the stability.

#123567 - $15.00 USD Received 29 Jan 2010; revised 7 Apr 2010; accepted 12 Apr 2010; published 20 Apr 2010

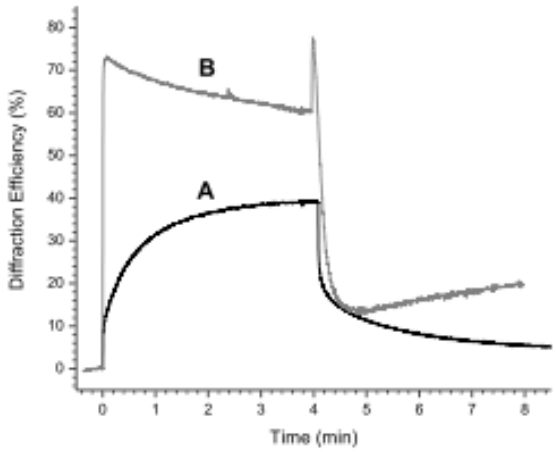

Fig. 3. Transient diffraction efficiency for Samples A (black) and B (gray). The voltage was 70V/μm for Sample B and 60V/μm for Sample A, since it could not withstand higher fields. The writing beams were turned on at $t = 0$ and were turned off after 4 minutes.

4. Theory and discussion

Observation of dynamic recovery in other systems has been associated with the formation of a competing grating via separate transport and trapping processes for holes and electrons [19–21]. Note that a grating from a single charge carrier is insufficient to explain the existence of two extrema in the decay without similar behavior also being present during formation. A useful theoretical model is provided by Bashaw *et al.* [22], developed for inorganic PR crystals. The SC field transients will rise and decay with two time constants. In general, however, the parameters for each rate depend on the recombination and ionization rates, mobilities, etc. of each charge species, and cannot be attributed separately to electrons and holes, except in the trap-limited case. That solution is

$$E_{sc}(t) = A_{+}e^{-\Gamma_{+}t} + A_{-}e^{-\Gamma_{-}t} \tag{1}$$

where Γ_{+} and Γ_{-} are the decay rates for each grating, and A_{+} and A_{-} contain the initial conditions and various material parameters, such as recombination and drift rates for electrons and holes. A similar solution is obtained for the SC field formation.

This result is adapted here to include a relative phase shift between the two gratings and to associate two time constants with one of the gratings. This latter modification is added because in PR polymers, both conduction and orientation contribute to the efficiency dynamics on different time scales, so multiple time constants are needed. It is incorporated only for one grating because it is clear from the transients that one grating is much faster than the other, so additional parameters to describe longer term behavior are not necessary. Thus, the equations for the time-dependence of the SC field and efficiency are as follows:

$$E_{SC}^{rise}(t) = E_1\left[\left(1-m\cdot e^{-\Gamma_{1s}t}-\left(1-m\right)\cdot e^{-\Gamma_{1l}t}\right)+\frac{E_2}{E_1}\left(1-e^{-\Gamma_{2s}t}\right)\cdot e^{-i\phi}\right] \tag{2}$$

$$E_{SC}^{decay}(t) = E_1\left[m\cdot e^{-\Gamma_{1s}t}+\left(1-m\right)\cdot e^{-\Gamma_{1l}t}+\frac{E_2}{E_1}\cdot e^{-\Gamma_{2s}t}\cdot e^{-i\phi}\right] \tag{3}$$

$$\eta(t) = \sin^2\left(c_1\left|\frac{E_{sc}(t)}{E_1}\right|\right). \tag{4}$$

#123567 - $15.00 USD Received 29 Jan 2010; revised 7 Apr 2010; accepted 12 Apr 2010; published 20 Apr 2010

(2) and (3) describe the rise and decay of the SC field, respectively. E_1 and E_2 are the steady-state magnitudes of the fields from each grating, Γ_{1s} and Γ_{1l} are the short and long time constants, respectively, for grating one, Γ_{2s} is the short time constant for grating two, m is the weighting factor to account for the relative contribution of conduction and orientation effects on the dynamics, and ϕ is the relative phase shift. In general, because the mobilities and trap densities for electrons and holes are different, they will not transport by the same amount, nor will they move completely to antinodes of the laser field. Thus, the phase shift may take values between 0 and π. (4) gives the expression for the diffraction efficiency in the transmission geometry. All other time independent parameters affecting the efficiency (e.g., initial conditions), besides the SC field, are contained within the constant c_1.

There are seven parameters in this model, which was used to fit the dynamics of Sample B. The phase shift and relative grating magnitudes should be the same for the rise and decay, so both regimes were fit in an iterative fashion. The results are shown in Fig. 4. For the rise from (2), the parameters are: $c_1 = 2.10$, $m = 0.82$, $\Gamma_{1s} = 4.5s^{-1}$, $\Gamma_{2s} = 0.00085s^{-1}$, $\Gamma_{1l} = 0.0095s^{-1}$, $E_2/E_1 = 0.22$, and $\phi = 0.70\pi$. For the decay from (3), the parameters are: $c_1 = 2.30$, $m = 0.62$, $\Gamma_{1s} = 0.15s^{-1}$, $\Gamma_{2s} = 4x10^{-5}s^{-1}$, $\Gamma_{1l} = 0.020s^{-1}$, $E_2/E_1 = 0.22$, and $\phi = 0.70\pi$.

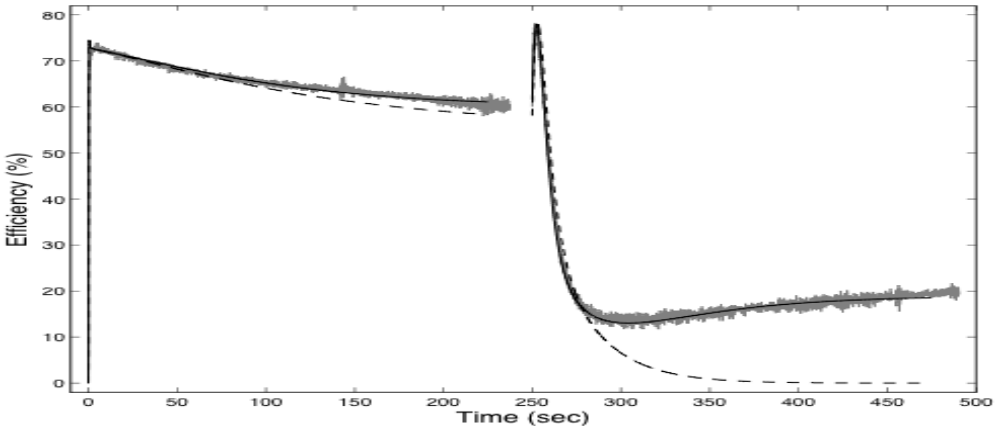

Fig. 4. Fit of the bipolar charge transport model to the transient efficiency data for Sample B. The gray curve is the data, the solid black curve is the best fit, and the dashed black curve is the best fit without the competing grating.

The physical processes are as follows. During writing, both a strong grating and a weak competing grating are formed. The decay in the signal is due primarily to the fact that the peak efficiency occurs at a lower modulation than what is achieved in the steady-state at 70V/μm. When the writing beams are turned off, the quick increase and decay is caused by the index modulation passing again through the over-modulation point. The stronger grating decays first and eventually becomes equal in magnitude to the weaker competing grating, which results in a minimum of the SC field (not exactly zero due to the phase shift). As the decay continues, the SC field reverses sign and the magnitude increases as the competing grating is slowly revealed. The dashed line in Fig. 4 is the best fit without the competing grating, showing the lack of recovery. Similarly, if only one decay constant is used for grating one, the theory predicts that the revelation of the second grating and recovery of efficiency would happen much faster than is observed, since the first grating decays more quickly. It is not possible to obtain as good a fit.

Based on experimental observations, we propose both hole and electron transport in this system. The HOMO and LUMO energies of the components are shown in Fig. 5 [17,23,24]. Hole transport occurs through the HOMO level of PATPD, and traps are provided by impurities, molecular conformations, and C_{60} anions. The electrons in the C_{60} will remain in the LUMO given the energies, but the electrons in 7-DCST can be trapped in either the Alq_3 or neutral C_{60}. Given that C_{60} has a higher molecular weight, smaller loading, and can be

#123567 - $15.00 USD Received 29 Jan 2010; revised 7 Apr 2010; accepted 12 Apr 2010; published 20 Apr 2010

reduced via illumination, the number density of Alq_3 is at least 4 times larger, and thus Alq_3 is the primary electron trap. Electrons can also be trapped in Alq_3 without having to transport to a dark region. Thus, there is a higher probability that charge pairs separate before recombination, increasing the magnitude of the primary grating leading to the improved steady-state performance, and allowing the SC field to develop to larger values in a shorter amount of time. This also allows both charge species to transport and trap, leading to the formation of two gratings. It is believed that the electron transport is occurring through the 7-DCST, though further tests are needed to confirm this.

The increased response time and efficiency is beneficial for many real-world applications, such as video rate displays and dynamic image correction. However, the long decay time of the competing grating limits speed without an erasing step. This can be overcome by writing for shorter times, which will still allow for efficient charge separation on short time scales while preventing the competing grating formation on longer time scales. However, in this composition, to make use of the effective increase in persistency the applications are limited to sufficiently long writing times.

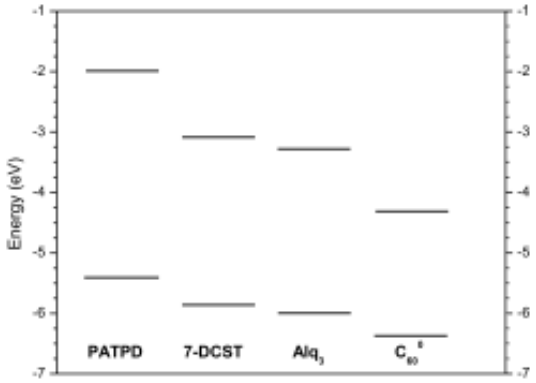

Fig. 5. Approximate location of HOMO and LUMO levels of the components.

The decreased photoconductivity (Fig. 6) in Sample B supports the interpretation of Alq_3 acting as an electron trap. Under illumination, both holes and electrons contribute to the current. Given the much larger concentration of the energetically favorable PATPD, Alq_3 is unlikely to affect the conduction of holes. This is also supported by the fact that Sample B tended to survive higher applied fields for much longer periods of time.

#123567 - $15.00 USD Received 29 Jan 2010; revised 7 Apr 2010; accepted 12 Apr 2010; published 20 Apr 2010

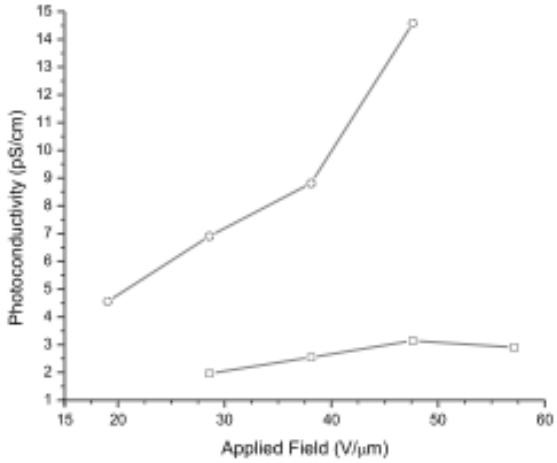

Fig. 6. Steady-state photoconductivity of Samples A (circles) and B (squares) versus applied field at 532nm. The 3-5 times smaller conductivity is due to the trapping of photo-generated electrons in Alq_3. The large increase in Sample A at about 50V/μm is likely due to the approaching breakdown.

5. Conclusion

The addition of Alq_3 to a photorefractive composite has been shown to increase the magnitude of two-beam coupling, reduce the over-modulation voltage, drastically increase the hologram writing speed, and allow the formation of a second, weaker grating via bipolar charge transport and trapping. In particular, Alq_3 doping can increase the sensitivity of PR polymers, improve the trap density necessary for reflection geometries and pulsed laser writing, and increase the dielectric breakdown strength, all of which can be limiting factors for real-world applications. This can have significant impact on several potential applications involving holography, such as telepresence, 3D entertainment, and industrial design.

Acknowledgements

The authors acknowledge support from the US Air Force Office of Scientific Research, the NSF Science and Technology Center for Materials and Devices for Information Technology Research Grant# - 0120967, and DARPA Phase II STTR.

#123567 - $15.00 USD Received 29 Jan 2010; revised 7 Apr 2010; accepted 12 Apr 2010; published 20 Apr 2010